Nanoscale

Accepted Manuscript

This article can be cited before page numbers have been issued, to do this please use: M. Martinez-Carmona, D. Lozano, A. Baeza, M. Colilla and M. Vallet-Regi, *Nanoscale*, 2017, DOI: 10.1039/C7NR05050J.

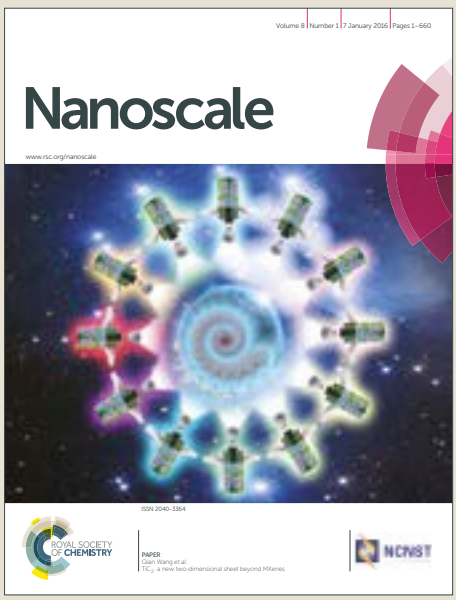




ROYAL SOCIETY OF CHEMISTRY

rsc.li/nanoscale

View Article Online
DOI: 10.1039/C7NR05050J

Nanoscale

ARTICLE

# A novel visible light responsive nanosystem for cancer treatment

M. Martínez-Carmona,[a,b*] D. Lozano,[a,b] A. Baeza,[a,b] M. Colilla[a,b] and M. Vallet-Regí[a,b*]

Received 00th January 20xx,
Accepted 00th January 20xx

DOI: 10.1039/x0xx00000x

www.rsc.org/

A novel singlet-oxygen sensitive drug delivery nanocarrier able to release their cargo after exposure to visible (Vis) light of a common lamp is presented. This nanodevice is based on mesoporous silica nanoparticles (MSN) decorated with porphyrin-caps grafted *via* reactive oxygen species (ROS)-cleavable linkages. In presence of Vis light the porphyrin-nanocaps produce singlet oxygen molecules that break the sensitive-linker, which triggers pore uncapping and therefore allows the release of the entrapped cargo (topotecan, TOP). This new system takes advantage of the non-toxicity and greater penetration capacity of Vis radiation and a double antitumor effect due to the drug release and the ROS production. *In vitro* tests with HOS osteosarcoma cancer cells reveal that TOP is able to be released in a controlled fashion inside the tumor cells. This research work constitutes a proof of concept that opens up promising expectations in the seeking for new alternatives for the treatment of cancer.

## Introduction

Due to its unique properties, especially its great loading capacity, mesoporous silica nanoparticles (MSN) have proven to be great candidates as nanocarriers for drug delivery purposes.[1–6] In recent years scientists have not only been focused on loading as much drug as possible but also on achieving a premature zero release system to avoid the appearance of undesirable side effects.[7] For this purpose several smart drug delivery nanodevices capable of releasing their cargo only after exposition to an internal or external stimulus have been designed.[8] Among the different stimuli (pH, enzymes, ultrasounds, magnetic fields, etc.), light is an excellent means to control the properties of materials and small molecules for many applications, especially when it is used for the controlled release of pharmacological agents for therapeutic purposes. The reason why light has emerged as one of the most promising alternatives is that its application can be spatial and timed controlled with ease.[9]

Since ultraviolet (UV) light has the highest power and can break bonds more easily than other radiations, it has been by far the most widely used radiation to trigger drug release from stimuli-responsive devices.[10–13] However, UV light has substantial drawbacks for *in vitro* and *in vivo* experiments and therefore for current medical applications. The first one concerns its low tissue penetrability (attenuation down to 1% occurs for light wavelengths of 250-280 nm at around 40 µm depth)[14] since many biological molecules absorb these energetic wavelengths directly. The second one is related to its toxicity. UV light causes progressive damage to human surrounded skin mediated by free radical generation[15], destruction of vitamins A,[16] and C,[17,18], collagen damage[19] and even worse genetic damage.[20] Therefore, systems able to respond to visible (Vis) light rather than to UV offer a less harmful alternative.[21] Vis light exhibits a more effective tissue penetrability (attenuation down to 1 % occurs up to 1.2 µm at 800 µm), which is ideal for medical applications. Besides, Vis light has a more innocuous nature due to a smaller energetic content. However, this lack of power is also responsible for its inefficiency when breaking bonds, and because of that, to date only a few visible light responsive devices have been reported.[22,23] However It has been observed that this energy is already enough to activate some photosensitizers in the production of reactive oxygen species (ROS).[24,25] ROS are highly reactive, especially with organic compounds that contain double bonds. It has been reported the spontaneous cleavage of aminoacrylates (β-enamino esters) following 2+2 cycloaddition reactions of singlet oxygen with olefins for the site-specific release of bioactive molecules.[26]

Herein, we propose and demonstrate an innovative approach to design a new Vis light-responsive drug delivery nanosystem. To this aim, the pore outlets of drug-loaded MSN are blocked via sol-gel chemistry by grafting silylated porphyrin nanocaps incorporating ROS-cleavable bonds, which have been carefully designed and whose synthesis has been optimized in this work. The irradiation of the nanosystem with Vis light would stimulate porphyrin nanocaps, generating ROS species able to

[a] *Dpto. Química Inorgánica y Bioinorgánica. Universidad Complutense de Madrid. Instituto de Investigación Sanitaria Hospital 12 de Octubre i+12. Plaza Ramón y Cajal s/n, 28040 Madrid, Spain.*
[b] *CIBER de Bioingeniería, Biomateriales y Nanomedicina, CIBER-BBN, Madrid, Spain.*
† *Corresponding author: M.V-R. vallet@ucm.es*
*Co-corresponding author: M.C. marinm11@ucm.es*
*Phone: +34 91 394 18 61; Fax: +34 91 394 17 90*

Electronic Supplementary Information (ESI) available: [H-NMR spectrum of the different steps of synthesis of the singlet oxygen labile linker, FTIR spectrum and Low-angle XRD patters of MSN and V-MSN, images of porphyrin/$[Ru(bipy)_3]^{2+}$ release and measurement of $[Ru(bipy)_3]^{2+}$ release in PBS in the presence/absence of visible light]. See DOI: 10.1039/x0xx00000x

break the sensitive bonds and therefore triggering pore uncapping and allowing drug release. The results derived from the current work constitute a significant advance in the nanomedicine field with potential application in cancer treatment.

## Experimental

### Reagents

Tetraethylorthosilicate (TEOS, 98%), n-cetyltrimethylammonium bromide (CTAB, ≥ 99%), sodium hydroxide (NaOH, ≥ 98%), ammonium nitrate ($NH_4NO_3$, ≥ 98%), propiolic acid (95%),4-piperidineacetic acid hydrochloride (PAH), (3-aminopropyl) triethoxysilane (APTES, ≥ 98%), N,N'-dicyclohexylcarbodiimide (DCC, 99%), N-hydroxysuccinimide (NHS, 98%), phosphate-buffered saline (PBS, 10x), phosphotungstic acid hydrate (PTA, reagent grade), tris(bipyridine)ruthenium(II) chloride ($[Ru(bipy)_3]Cl_2$), topotecan (TOP) and calcein (CAL) were purchased from Sigma-Aldrich (St. Louis, USA). 5,10,15,20-(Tetra-3-hydroxyphenl) porphyrin was purchased from Porphychem (Dijon, France). All other chemicals were purchased from Panreac Química SLU (Castellar del Valles, Barcelona, Spain) inc: absolute ethanol (EtOH), acetone, dimethyl sulfoxide (DMSO), tetrahydrofuran (THF), etc. All reagents were used as received without further purification. Ultrapure deionized water with resistivity of 18.2 MΩ was obtained using a Millipore Milli-Q plus system (Millipore S.A.S, Molsheim, France).

### Characterisation techniques

Powder X-Ray Diffraction (XRD) experiments were performed in a Philips X'Pert diffractometer equipped with Cu Kα radiation (wavelength 1.5406 Å) (Philips Electronics NV, Eindhoven, Netherlands). XRD patterns were collected in the 2θ range between 0.6° and 8° with a step size of 0.02° and counting time of 5 s per step. Thermogravimetric analysis (TGA) were performed in a Perkin Elmer Pyris Diamond TG/DTA (California, USA), with 5 °C $min^{-1}$ heating ramps, from room temperature (RT) to 600 °C. Fourier transform infrared spectroscopy (FTIR) was carried out in a Nicolet (Thermo Fisher Scientific, Waltham, MA, USA) Nexus spectrometer equipped with a Goldengate attenuated total reflectance (ATR) accessory (Thermo Electron Scientific Instruments LLC, Madison, WI USA). Morphology, mesoestructural order and nanoparticles functionalization were studied by High Resolution Transmission Electron Microscopy (HRTEM) with a JEOL JEM 3000F instrument operating at 300 kV, equipped with a CCD camera (JEOL Ltd., Tokyo, Japan). Sample preparation was performed by dispersing in ethanol and subsequent deposition onto carbon-coated copper grids. A 1% PTA solution (pH 7.0) was used as staining agent in order to visualize the organic coating around MSN.

To determine the evolution of the size and surface charge of nanoparticles by dynamic light scattering (DLS) and zeta (ζ)-potential measurements, respectively, a Zetasizer Nano ZS (Malvern Instruments, United Kingdom) equipped with a 633 nm "red" laser 7 was used. DLS measurements were directly recorded in ethanolic colloidal suspensions. ζ-potential measurements were recorded in aqueous colloidal suspensions. For this purpose 1 mg of nanoparticles was added to 10 mL of solvent followed by 5 min of sonication to obtain a homogeneous suspension. In both cases measurements were recorded by placing 1 mL of suspension (0.1 mg $mL^{-1}$) in DTS1070 disposable folded capillary cells (Malvern Instruments). The textural properties of the materials were determined by $N_2$ adsorption porosimetry by using a Micromeritics ASAP 2020 (Micromeritics Co., Norcross, USA). To perform the $N_2$ measurements, 20-30 mg of each sample was previously degassed under vacuum for 24 h at 40 °C. The surface area ($S_{BET}$) was determined using the Brunauer-Emmett-Teller (BET) method and the pore volume ($V_P$) was estimated from the amount of $N_2$ adsorbed at a relative pressure around 0.97. The pore size distribution between 0.5 and 40 nm was calculated from the adsorption branch of the isotherm by means of the Barrett-Joyner-Halenda (BJH) method. The mesopore size ($D_P$) was determined from the maximum of the pore size distribution curve. Nuclear magnetic resonance (NMR) measurements were performed in a Bruker AV250 spectrometer (Karlsruhe, Germany).

### Synthesis of mesoporous silica nanoparticles (MSN)

Bare MSN, denoted as MSN, were synthesized by the modified Stöber method using TEOS as silica source in the presence of CTAB as structure directing agent. Briefly, 1 g of CTAB, 480 mL of $H_2O$ and 3.5 mL of NaOH (2 M) were added to a 1,000 mL round bottom flask. The mixture was heated to 80 °C and magnetically stirred at 600 rpm. When the reaction mixture was stabilized at 80 °C, 5 mL of TEOS were added dropwise at 0.33 mL $min^{-1}$ rate. The obtained white suspension was stirred for further 2h at 80 °C. The reaction mixture was centrifuged and washed three times with water and ethanol. Then the surfactant was removed by ionic exchange by soaking 1 g of nanoparticles in 500 mL of a $NH_4NO_3$ solution (10 mg $mL^{-1}$) in ethanol (95%) at 65 °C overnight under magnetic stirring. The nanoparticles were collected by centrifugation, washed twice with water and twice with ethanol and stored in ethanol.

### Synthesis of singlet oxygen-labile linker

The synthesis of the singlet oxygen-labile linker was carried out in several steps and always under $N_2$ atmosphere and in the absence of light. Firstly to a 0.5 mL of an ice cooled and stirred solution of porphyrin (25 mg, 0.036 mmol) and propiolic acid (12 µL, 0.18 mmol) in dry THF, a solution of 0.5 mL of *N,N'*-dicyclohexylcarbodiimide (DCC, 37.6 mg, 0.18 mmol) and 4-dimethylaminopyridine (DMAP, 2 mg, 0.016 mmol) was added dropwise during 15 min. Reaction mixture was then stirred overnight at RT.

At the same time, a mixture of 4-piperidineacetic acid hydrochloride (26 mg), DCC (7.28 mg) and NHS (4 mg) was dissolved in 2 mL of dry DMSO and left to react for 5 h before

adding APTES (34 µL, 0.18 mmol) and leaving it to react overnight.
Finally both solutions were mixed during 24 h to get the desired linker.

**[Ru(bipy)$_3$]Cl$_2$/topotecan (TOP)/calcein (CAL) loading**

25 mg of MSN was placed in a topaz vial and then, 3 mL of a 14 mg mL$^{-1}$ EtOH solution of [Ru(bipy)$_3$]Cl$_2$ (RBP), or an aqueous solution of CAL or TOP (6 or 9 mg mL$^{-1}$, respectively) was added and the suspension was stirred at room temperature for 24 h. The sample was centrifuged and the nanoparticles were resuspended in 500 mL of EtOH and placed in a 3-necked round flask.

**Attachment of the singlet oxygen-labile linker on the MSN**

25 mg of MSN was placed in a 3-necked round bottom flask and dried under vacuum. Then, 5 mL of dry toluene was added and the flask was placed in an ultrasonic bath for a better suspension of the particles. Subsequently, the solution of the singlet oxygen-labile linker previously prepared was added keeping the reaction in the darkness under a nitrogen atmosphere at 80 °C for 24 h. Then, the reaction mixture was centrifuged and washed three times with DMSO, two times with EtOH and two times with water. Finally, the product was resuspended in 3 mL of PBS 1x.

***In vial* cargo release assays**

To investigate the light-responsive drug release performance of V-MSN, TOP was chosen as a potent cytotoxic drug and *in vial* time-based fluorescence release experiments in presence and absence of visible light (20 W bulb) were carried out. Two batches of 400 µL of 8.33 mg mL$^{-1}$ of TOP-loaded V-MSN (V-MSN@TOP) suspension were placed in a vial. One of them was exposed to Vis light irradiation for 30 min while orbital stirring. The other batch was treated under similar conditions but without light irradiation.
For the release experiments, the procedure reported by Bein and coworkers was used.[27] Thus, 170 µL of each nanoparticles suspension was filled into a reservoir cap sealed with a dialysis membrane (molecular weight cut-off 12,000 g mol$^{-1}$), allowing released dye molecules to pass into the fluorescence cuvette (which was completely filled with PBS 1x) while the relatively large particles were held back. Experiments were performed at a temperature of 37 °C. The amount of drug released was determined by fluorescence measurements of the solutions recorded on a PTI QuantaMaster 400 system featuring a JYF-FLUOROMAX-4 compact spectrofluorimeter single grating excitation and emission monochromator with a photomultiplier detector (PMT R928P) and an automated four-position thermostated cuvette-holder (FL-1011) (PTI, Photon Technology International, HORIBA Jobin Yvon GmbH, Germany). For temperature settings, a MTB-IFI-156-5251 refrigerated bath circulator with a peltier was used. TOP was excited with $\lambda_{exc}$ = 400 nm and showed a maximum of emission at $\lambda_{em}$ = 540 nm (excitation slit 0.38 mm, emission slit 0.38 mm, integration 1s).

***In vitro* cell culture**

Cell culture studies were performed using HOS cells derived from a human osteosarcoma. The tested MSN (50 µg mL$^{-1}$) were placed into each well of 24-well plates after cell seeding. HOS cells were then plated at a density of 20.000 cells cm$^2$ in Dulbecco's modified Eagle's medium (DMEM, Sigma Chemical Company), respectively, containing 10% of heat-inactivated fetal bovine serum and 1% penicillin– streptomycin at 37 °C in a humidified atmosphere of 5% $CO_2$, and incubated for different times. Some wells contained no MSN as controls.

**Cell viability**

Cell proliferation was assessed after HOS cell incubation in 24-well plates with MSN for 24 and 48h. The tested MSN (50 µg mL$^{-1}$) were placed during 2 h. Cells were then exposed or not (same conditions) to visible light irradiation for 30 min with orbital stirring. Cells were washed with PBS three times. At 24 h and 48 h, Alamar Blue solution (AbD Serotec, Oxford, UK) at 10% (v/v) was added to the cell culture. 4 h thereafter, absorbance was measured using excitation and emission wavelengths of 540 and 620 nm, respectively.

**Fluorescence microscopy**

Cells were incubated with the CAL loaded MSN (V-MSN@CAL) (50µg mL$^{-1}$) for 2h in serum-free culture medium. Cells were then exposed or not (same conditions) to Vis light irradiation for 30 min under orbital stirring. Then, the medium was withdrawn and cells were washed with PBS three times and the medium was replaced. At 1h, cells were fixed with ethanol. Fluorescence microscopy images were taken to evaluate intracellular calcein release essay. Green channel was used to locate the calcein release in an Evos FL Cell Imaging System equipped with tree Led Lights Cubes (lEX (nm); lEM (nm)): DAPY (357/44; 447/60), GFP (470/22; 525/50), RFP (531/40; 593/40) from AMG (Advance Microscopy Group).

## Results and discussion

Vis light-responsive mesoporous silica nanoparticles (V-MSN) were composed of porphyrin caps, able to generate singlet oxygen by irradiation of Vis light, covalently grafted to the surface of MCM-41 type MSN by (β-enamino esters), a singlet oxygen-labile linker. The synthesis and characterization of MSN had been previously reported,[28] and their high loading capacity was took in advance for loading TOP. Then, the pores were closed with a Vis light-responsive system to avoid premature release (Figure 1).

**Synthesis of the visible light-responsive system**

The synthesis of the photosensitive system was carried out in several steps and always under $N_2$ atmosphere and absence of light (Figure 2).

Firstly, the singlet oxygen-labile linker was synthesized, and the structure of each reaction intermediate was confirmed by $^1$H-NMR. The HO-porphyrin was coupled with propiolic acid using the Steglich esterification reaction. The presence of a singlet at 3.792 ppm characteristic of the propiolic acid confirmed that the obtained product was "A" (S1). In the reaction between APTES and 4-piperidineacetic acid hydrochloride (PAH), the

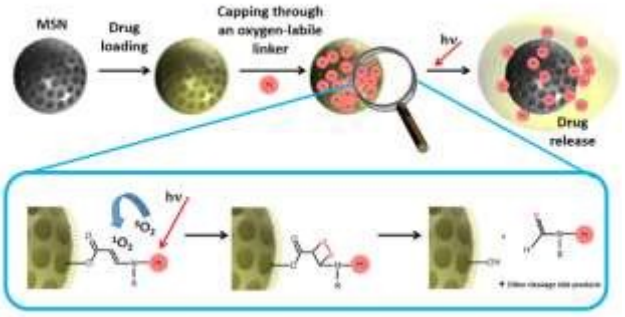


**Figure 1.** Schematic depiction illustrating the operation mechanism of the nanodevice developed in this work.

appearance of a new signal at 7.965 ppm due to amide formation between the amino group of the APTES and the carboxylic acid of the PAH was observed, giving place to product "B" (S2). Finally, after the reaction between products "A" and "B" the complete singlet oxygen-labile linker was obtained. A proof of this fact was the disappearance of the singlet signal corresponding to the alkyne protons and the appearance of two doublets due to the protons of the formed double bond (S3). Due to the complexity of the product, and to ensure that the assignment was correct, a parallel and simpler reaction was performed where "A" was reacted with PAH ("C"). In this case the appearance of the double bonds (S4) and their relation through a COSY spectrum (S5) were better observed.

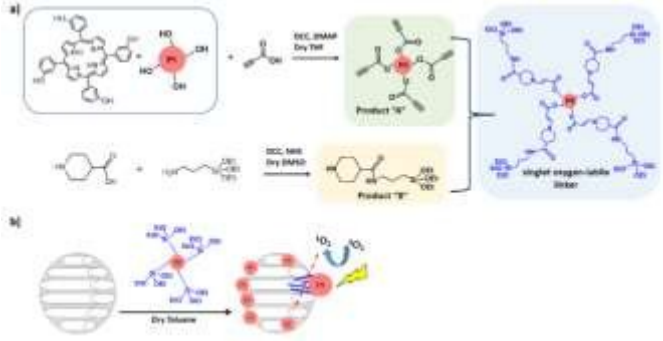

**Figure 2.** Scheme of **a)** synthesis of singlet oxygen-labile linker and **b)** attachment of the synthetized linker on the MSN.

In order to evaluate the sensitive nature of this double bond to oxidation by singlet oxygen, the resulted compound was irradiated with a desk lamp for 30 min. The reaction of olefins with singlet oxygen was monitored by the decrease of olefinic proton peaks in the $^1$H-NMR spectra (Figure 3).

View Article Online
DOI: 10.1039/C7NR05059J

Once again we compared this response with that obtained for the simpler system "C" to visualize the bond rupture in an easier way (S6).

Once the formation and functionality of the singlet oxygen-labile linker was confirmed it was used to decorate the MSN surface by refluxing in dry toluene for 12 h in the darkness, producing the functionalized particles V-MSN.

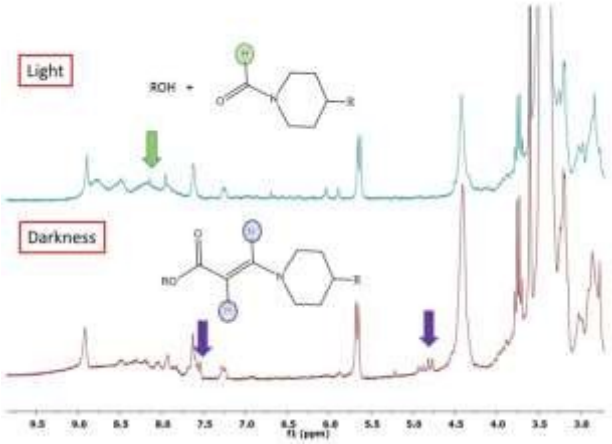


**Figure 3.** $^1$H-NMR spectra of the photo-oxidation of the singlet oxygen-labile linker.

The resulting material was deeply characterized by different techniques. The change from a clean FTIR spectrum in the 1500–2000 $cm^{-1}$ range of MSN to the presence of several bands at 1624 $cm^{-1}$ and 1454 $cm^{-1}$ due to the amide bond formation and the C=C stretching of the aromatic rings corroborated the functionalization (S7).[29] The difference between TGA measurements of V-MSN and MSN indicated a functionalization degree of 17%.

The textural properties of the nanoparticles, mainly the surface area ($S_{BET}$), pore volume ($V_P$) and pore diameter ($D_P$), derived from the treatment of $N_2$ adsorption measurement data, experienced noticeable reduction after surface decoration. Thus the $S_{BET}$ decreases from 1116 $m^2\ g^{-1}$ for MSN to 458 $m^2\ g^{-1}$ for V-MSN. The initial $V_P$ of MSN dropped from 1.05 $cm^3\ g^{-1}$ to 0.22 $cm^3\ g^{-1}$ for V-MSN. Finally, the $D_P$ also suffers a decrease from 2.9 nm for MSN to 1.9 nm for V-MSN.

The ζ-potential value of the nanoparticles in water experienced a noticeable change from -34.6 ± 0.01 for MSN to -20.7 ± 0.04 for V-MSN due to a decrease in the number of surface silanol groups. The disappearance of two of the characteristics signals (11 and 20) of the XRD patters of MSN in the coated nanoparticles (S8) may be also ascribed to the partial filling of the mesopore channels by the functionalization agent, as reported elsewhere.[30,31]

View Article Online
DOI: 10.1039/C7NR05050J



TEM images of MSN showed a honeycomb mesoporous arrangement typical of MCM-41 (Figure 4).
Grafting of the photolinker did not affect the mesostructural order of V-MSN. The morphology of the nanoparticles was also preserved, showing spherical particles in both cases. Finally, the transition from a smooth (MSN) to a rough (V-MSN) particle surface, due to the capping shell was clearly observed (Figure 4). The average diameter of the nanosystems, estimated from the measurement of 20 nanoparticles was *ca.* 110 nm and 130 nm for MSN and V-MSN, respectively, with a relative error of *ca.* 10%.

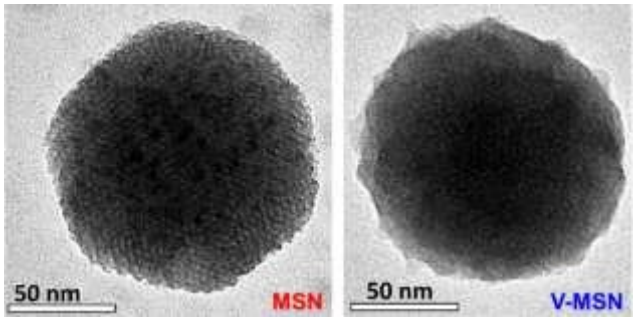


**Figure 4.** TEM images of MSN and V-MSN. Samples were stained with 1% PTA.

**Response to light**

The first step was to check if after being anchored to the nanoparticle the linker remained sensitive to the action of Vis light. For this purpose, and due to the lack of solubility of porphyrin in water, 10 mg of V-MSN were weighed, suspended in 2 mL of DMSO and divided into 2 vials. One was exposed to light from a lamp for 30 min with orbital stirring while the second was exposed to the same conditions but protected from light as a control. Afterwards, both samples were centrifuged. A clearly colored supernatant was observed due to the release of the porphyrin in the case of the sample subjected to light and a colourless supernatant for the sample that remained in darkness (S9a).
After proving the Vis light-responsive behaviour, the effectiveness of the capping was studied. Hence 25 mg of MSN were loaded with $[Ru(bipy)_3]Cl_2$ as the fluorophore for 24 h. Subsequently, the particles were capped with the singlet oxygen-labile linker as previously described, affording (V-MSN@RBPY). Two batches of V-MSN@RBPY were suspended in water and one of them was exposed to irradiation for 30 min under stirring. The other batch was treated under similar conditions but without light irradiation. Then, 170 µL of each suspension was filled into a reservoir cap sealed with a dialysis membrane, allowing released dye molecules to pass into the fluorescence cuvette (which was completely filled with PBS at pH 7.4). The amount of fluorophore released was determined by fluorescence measurements of the solutions, ($\lambda_{ex}$ = 451 nm, $\lambda_{em}$ = 619 nm). The dye released for the irradiated and non-irradiated V-MSN@RBPY sample is shown in S9b showing a remarkable fluorescence increase in the case of the illuminated sample once the experiment was concluded (S9c).
Afterwards the experiment was repeated but in this case using V-MSN@TOP nanoparticles. The estimated amount of TOP loaded into the nanosystem was found to be 5.3% in weight, as determined from the differences between the fluorescence measurements of the initial and the recovered filtrate solutions. In this case, the drug release was monitored by fluorescence excitation spectroscopy under continuous settings during 18 h (Figure 5).

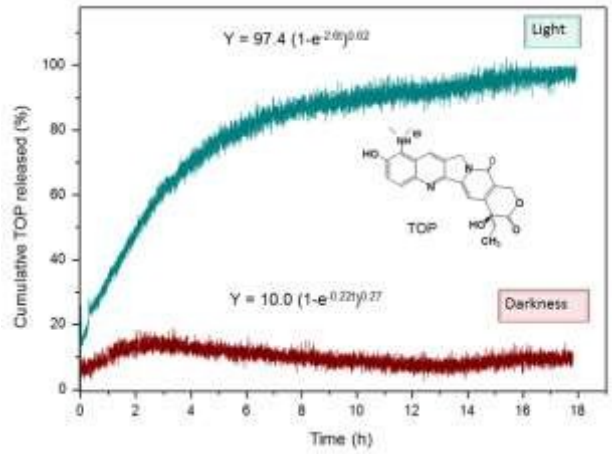


**Figure 5.** *In vial* drug release profiles from V-MSN@TOP in the absence of light (darkness) and upon visible light irradiation (light).

Release profiles can be adjusted to first-order kinetic model by introducing an empirical non-ideality factor (δ) to give the following equation:[32]

$$Y = A(1 - e^{-kt})^{\delta}$$

being Y the percentage of TOP released at time *t*, *A* the maximum amount of drug released (in percentage), and *k*, the release rate constant. The values for $\delta$ are comprised between 1 for materials that obeys first-order kinetics, and 0, for materials that release the loaded cargo in the very initial time of test. The parameters of the kinetic fitting shown in Figure 5 ($R^2$ = 0.990) indicate that, whereas the maximum amount of TOP released is practically the totality of the loaded drug after light irradiation, almost negligible is released under darkness conditions.
After Vis light irradiation the $\delta$ value was 0.62, pointing to a near first order kinetics with certain contribution of an initial burst release of the entrapped molecules. On the contrary, nanoparticles not exposed to light, exhibited a δ value of 0.27, indicating that the small amount of TOP released could be due to the release of TOP located within uncapped channels and

not in the mesopores, whose release was successfully hindered by the capping of the pore entrances with the porphyrin-derivatized linker. Actually, the total cargo release was almost 10-fold higher for irradiated V-MSN@TOP nanoparticles than for non-irradiated ones, which was associated to a *k* value more than ten times greater in irradiated sample. This finding can be explained by the cleavage of the visible-light breakable linkages of the pore capping agent after irradiation, which would trigger the removal of the porphyrin nanocaps and would allow the departure of the entrapped molecules.

### *In vitro* cytotoxicity evaluation

First of all, we confirmed that exposure of HOS cells to 30 min of Vis light irradiation induce a significant decrease (15-20%) in cell viability in presence of V-MSN. No differences in viability were observed when HOS cells without V-MSN were exposed to visible light irradiation (results not shown) in the same conditions. After that, we studied the cytotoxicity of the system. HOS cells were cultured for 2 h with the nanoparticles (50 μg $mL^{-1}$) loaded or not with TOP, V-MSN(@TOP), and then washed to eliminate the non-internalized particles. After that, part of the cells were irradiated with Vis light for 30 min while the others remained in darkness. Vis light irradiation only produces a 15% of death in HOS cells that contain drug-free V-MSN at 24 h of cell culture, probably due to the production of ROS[33] (Figure 6a). While Vis light irradiation of V-MSN@TOP induced a significant decreased in HOS viability at 24 h (30%) and 48 h (50%) of cell culture. (Figure 6b). The effect of free TOP has not been evaluated due to its known inactivation under neutral conditions.[31,34,35]

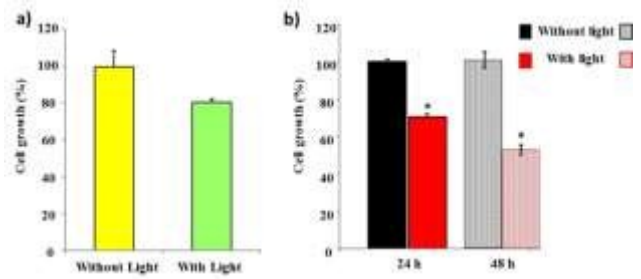


**Figure 6.** HOS viability in presence or absence of Vis light irradiation (30 min) (a) with V-MSN at 24 h of cell culture and (b) with V-MSN@TOP (50 μg $mL^{-1}$) at 24h and 48h of cell culture after presence or absence of visible light irradiation (30 min), measured by Alamar Blue solution. Results are mean ± SE of three independent experiments performed in triplicate. p <0.05 *vs* corresponding control (student's t-test).

### Intracellular calcein release essay

It is well known that one of the major challenges when designing nanodevices is that some drugs are not able to cross the cell membrane and therefore are locked inside the endosomes what greatly limit their effectiveness. Our system has porphyrin as a cap so that it is able to produce ROS that favours the drug endosome escape and the cytoplasm reach.[36] To probe that, V-MSN were loaded with CAL (V-MSN@CAL), that as has been studied[37,38] is a membrane impermeable molecule, and incubated with HOS cells for 2h. The media were changed and the samples showed a perinuclear location of the nanoparticles that seems to indicate the V-MSN@CAL uptaken by the cells. After 24h the cells exhibited a dot-like pattern indicating that CAL was still inside the nanoparticles (Figure 7a).

However, 1h after the photoactivation the green fluorescence was through the entire cell proving unequivocally, that the nanogates of the pores were opened and the CAL escape from the endosome. (Figure 7b).

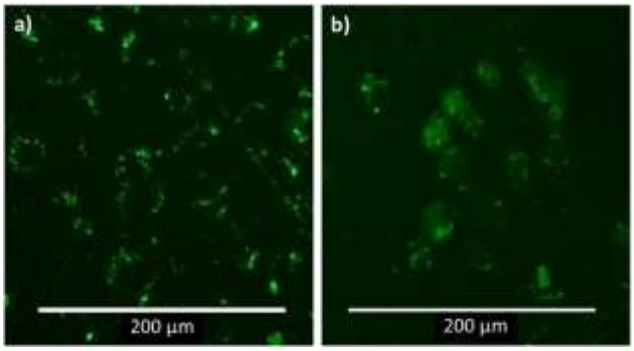


**Figure 7.** *Fluorescence microscopy images of HOS cells incubated with V-MSN@CAL loaded before (a) and after (b) light irradiation.*

## Conclusions

In conclusion, we have successfully proved a novel nanomaterial able to transport topotecan and release it in response to visible light irradiation. In this device the porphyrin acts both as cap and bond breaker trigger via photo-unclick chemistry. Almost 99% of the cargo is released after 18 h after being submitted to 30 min of irradiation with very low intensity light. Besides the action of the drug itself the generation of ROS favours the antitumor effect of the system. The cytotoxic capacity of this system was evaluated in vitro against tumour cell lines showing an excellent performance as it was able to transform the diseased cells into apoptotic cells using a very low particle dose.

This demonstrates that our drug delivery system can be used to efficiently transport membrane impermeable cargos into the cell.

Since the release can be triggered by visible light, the two main ultraviolet light drawbacks, low penetrability and harmfulness, are overcome. This proof of concept reveals the tremendous potential of our system as a valuable tool for its application in the spatial-temporal release of not only drugs but also other bioactive molecules. Therefore it is envisioned as a new

alternative for the treatment of cancer and many other diseases.

## Acknowledgements

The authors thank financial support from European Research Council [ERC-2015-AdG-694160 (VERDI)] and Ministerio de Economía y Competitividad, Spain (Project MAT2015-64831-R). The XRD measurements, $^{1}H \rightarrow {}^{13}C$ solid-state NMR spectra and internalisation studies were performed at C.A.I. Difracción de Rayos X, C.A.I. Resonancia Magnética Nuclear and C.A.I. Citometría de Flujo from UCM (Spain), respectively. TEM studies were performed at ICTS National Centre for Electron Microscopy (Spain).

## References

1 M. Vallet-Regí, F. Balas and D. Arcos, *Angew. Chem. Int. Ed. Engl.*, 2007, **46**, 7548–58.

2 M. Vallet-Regí, A. Rámila, R. P. del Real and J. Pérez-Pariente, *Chem. Mater.*, 2001, **13**, 308–311.

3 C. Argyo, V. Weiss, C. Bra and T. Bein, *Chem. Eur. J.*, 2013, **26**, 435–451.

4 A. Popat, S. B. Hartono, F. Stahr, J. Liu, S. Z. Qiao and G. Qing (Max) Lu, *Nanoscale*, 2011, **3**, 2801–2818.

5 J. L. Vivero-Escoto, I. I. Slowing, B. G. Trewyn and V. S.-Y. Lin, *Small*, 2010, **6**, 1952–1967.

6 Z. Li, J. C. Barnes, A. Bosoy, J. F. Stoddart and J. I. Zink, *Chem. Soc. Rev.*, 2012, **41**, 2590–2605.

7 D. A. Scheinberg, C. H. Villa, F. E. Escorcia and M. R. McDevitt, *Nat. Rev. Clin. Oncol.*, 2010, **7**, 266–276.

8 M. Martínez-Carmona, M. Colilla and M. Vallet-regí, *Nanomaterials*, 2015, 1906–1937.

9 J. M. Morachis, E. A. Mahmoud and A. Almutairi, *Pharmacol. Rev.*, 2012, **64**, 505–519.

10 M. Martínez-Carmona, A. Baeza, M. A. Rodriguez-Milla, J. Garcia-Castro and M. Vallet-Regí, *J. Mater. Chem. B*, 2015, **3**, 5746–5752.

11 N. Ž. Knežević and V. S.-Y. Lin, *Nanoscale*, 2013, **5**, 1544–51.

12 N. K. Mal, M. Fujiwara and Y. Tanaka, *Nature*, 2003, **421**, 350–353.

13 Q. Jin, F. Mitschang and S. Agarwal, *Biomacromolecules*, 2011, **12**, 3684–3691.

14 Scientific Committee on Emerging and Newly-Identified Health Risks, *The appropriateness of the risk assessment methodology in accordance with the Technical Guidance Documents for new and existing substances for assessing the risks of nanomaterials*, 2012.

15 B. A. Jurkiewicz, R. B. U. E. Tner and R. Buettner, *Photochem. Photobiol.*, 1994, **59**, 1–4.

16 Z. Wang, M. Boudjelal and S. Kang, *Nat. Med.*, 1999, **5**, 0–4.

17 M. Podda, M. G. Traber, C. Weber, L. J. Yan and L. Packer, *Free Radic. Biol. Med.*, 1998, **24**, 55–65.

18 Y. Shindo, E. Witt and L. Packer, *J. Invest. Dermatol.*, 1993, **100**, 260–265.

19 K. Jariashvili, B. Madhan, B. Brodsky, A. Kuchava, L. Namicheishvili and N. Metreveli, *Biopolymers*, 2012, **97**, 189–198.

20 R. P. Sinha and D.-P. Häder, *Photochem. Photobiol. Sci.*, 2002, **1**, 225–236.

21 J. Olejniczak, C. J. Carling and A. Almutairi, *J. Control. Release*, 2015, **219**, 18–30.

22 N. Z. Knezevic, B. G. Trewyn and V. S. Y. Lin, *Chem. Commun.*, 2011, **47**, 2817–2819.

23 C. Carling, M. L. Viger, A. Nguyen, V. Garcia and A. Almutairi, *Chem. Sci.*, 2014, **6**, 335–341.

24 A. S. Lavado, V. M. Chauhan, A. Alhaj Zen, F. Giuntini, D. R. E. Jones, R. W. Boyle, A. Beeby, W. C. Chan and J. W. Aylott, *Nanoscale*, 2015, **7**, 14525–14531.

25 H. Kolarova, P. Nevrelova, K. Tomankova, P. Kolar, R. Bajgar and J. Mosinger, *Gen. Physiol. Biophys.*, 2008, **27**, 101–105.

26 M. Y. Jiang and D. Dolphin, *J. Am. Chem. Soc.*, 2008, **130**, 4236–7.

27 A. Schlossbauer, J. Kecht and T. Bein, *Angew. Chemie-International Ed.*, 2009, **48**, 3092–3095.

28 J. S. Beck, J. C. Vartuli, W. J. Roth, M. E. Leonowicz, C. T. Kresge, K. D. Schmitt, C. T. W. Chu, D. H. Olson, E. W. Sheppard, S. B. McCullen, J. B. Higgins and J. L. Schlenker, *J. Am. Chem. Soc.*, 1992, **114**, 10834–10843.

29 James O. Alben, S. S. Choi, A. D. Adler and W. S. Caughey, *Ann. N. Y. Acad. Sci.*, 1973, **206**, 278–295.

30 O. Terasaki, T. Ohsuna, Z. Liu, Y. Sakamoto and A. E. Garcia-Bennett, *Stud. Surf. Sci. Catal.*, 2004, **148**, 261–288.

31 M. Martínez-Carmona, D. Lozano, M. Colilla and M. Vallet-Regí, *RSC Adv.*, 2016, **6**, 50923–50932.

32 F. Balas, M. Manzano and M. Vallet-Regí, *Acta Biomater.*, 2008, **4**, 514–522.

33 P. Agostinis, K. Berg, K. A. Cengel, T. H. Foster, A. W. Girotti, S. O. Gollnick, S. M. Hahn, M. R. Hamblin, A. Juzeniene, D. Kessel, M. Korbelik, J. Moan, P. Mroz, D. Nowis, J. Piette, B. C. Wilson and J. Golab, *CA. Cancer J. Clin.*, 2011, **61**, 250–281.

34 V. M. M. Herben, W. W. ten Bokkel Huinink and J. H. Beijnen, *Clin. Pharmacokinet.*, 1996, **31**, 85–102.

35 P. Tardi, E. Choice, D. Masin, T. Redelmeier, M. Bally and T. D. Madden, *Cancer Res.*, 2000, **60**, 3389–3393.

36 A. M. Sauer, A. Schlossbauer, N. Ruthardt, V. Cauda, T. Bein and C. Bräuchle, *Nano Lett.*, 2010, **10**, 3684–3691.

37 S. A. Mackowiak, A. Schmidt, V. Weiss, C. Argyo, C. Von Schirnding, T. Bein and C. Bräuchle, *Nano Lett.*, 2013, **13**, 2576–2583.

38 J. L. Paris, M. V. Cabanas, M. Manzano and M. Vallet-Regí, *ACS Nano*, 2015, **9**, 11023–11033.

View Article Online
DOI: 10.1039/C7NR05050J